Wind and Structures, *Vol. 21, No. 6 (2015) 677-691*
DOI: http://dx.doi.org/10.12989/was.2015.21.6.677

Vibration-based identification of rotating blades using Rodrigues' rotation formula from a 3-D measurement

Chin-Hsiung Loh[*1], Yu-Ting Huang[1a], Wan-Ying Hsiung[1b], Yuan-Sen Yang[2c] and Kenneth J. Loh[3d]

[1]*Department of Civil Engineering, National Taiwan University, Taipei 10617, Taiwan*
[2]*Department of Civil Engineering, National Taipei University of Technology, Taipei, Taiwan*
[3]*Department of Structural Engineering, University of California at San Diego, La Jolla, CA 92093, USA*

(Received September 3, 2015, Revised December 4, 2015, Accepted December 6, 2015)

Abstract. In this study, the geometrical setup of a turbine blade is tracked. A research-scale rotating turbine blade system is setup with a single 3-axes accelerometer mounted on one of the blades. The turbine system is rotated by a controlled motor. The tilt and rolling angles of the rotating blade under operating conditions are determined from the response measurement of the single accelerometer. Data acquisition is achieved using a prototype wireless sensing system. First, the Rodrigues' rotation formula and an optimization algorithm are used to track the blade rolling angle and pitching angles of the turbine blade system. In addition, the blade flapwise natural frequency is identified by removing the rotation-related response induced by gravity and centrifuge force. To verify the result of calculations, a covariance-driven stochastic subspace identification method (SSI-COV) is applied to the vibration measurements of the blades to determine the system natural frequencies. It is thus proven that by using a single sensor and through a series of coordinate transformations and the Rodrigues' rotation formula, the geometrical setup of the blade can be tracked and the blade flapwise vibration frequency can be determined successfully.

Keywords: signal processing; stochastic subspace identification; Rodrigues' rotation formula; wireless sensing system; a research-scale turbine blade system

1. Introduction

A wind turbine system consists of a connected and a flexible sub-entity, namely, a tower and a rotor system comprising three rotating blades, and these entities are characterized by the effects of the tower/blade interaction. As per Barlas *et al*. (2010), the loads acting on a wind turbine during normal operation can be classified into aerodynamic and gravitational (external) as well as structural loads (internal), which are related by aero-elastic coupling. Two main types of vibration occur in wind turbine blades: flapwise and edgewise. Flapwise vibrations occur out of the rotor

∗Corresponding author, Professor, E-mail: lohc0220@ccms.ntu.edu.tw
[a] Graduate Student, E-mail: r01521228@ntu.edu.tw
[b] Graduate Student, E-mail: r01521205@ntu.edu.tw
[c] Associate Professor, E-mail: vin389@gmail.com
[d]Associate Professor, E-mail: kenloh@ucsd.edu

http://www.techno-press.org/?journal=was&subpage=8 ISSN: 1226-6116 (Print), 1598-6225 (Online)

plane, whereas edgewise vibrations occur in the rotor plane. The flapwise vibration is similar to the phenomenon of fluttering in aircraft wings and, in extreme cases, leads to collision of the turbine blades with the tower, resulting in catastrophic failure of the structure.

Theoretical studies on the dynamic characteristics of a rotating blade indicate two physical phenomena that influence the flapwise blade vibration characteristics: centrifugal stiffening caused by blade rotation and the gravitational force acting on the blade. In addition, the geometrical setup of the blade system, including the pitching, rolling, and tilt angles of rotating blades, may influence the vibration characteristics of blades in both flapwise and edgewise directions. Tracking of the geometric setup of a turbine blade system and determining the dynamic characteristics of a wind turbine during operation require appropriate techniques for determining the dynamic behavior of a turbine blade, cyclic effects of the vibration response, and structural modes of a rotating turbine. Ness *et al.* (1996) provided a handbook of various existing nondestructive testing techniques, including visual inspection, acoustic emission technique, and stereography detection of composite blade damage. James III et al. (1996) investigated several structural damage detection techniques using vibration measurements. Simmermacher *et al.* (1997) proposed a structural health monitoring technique for wind turbines. Lading *et al.* (2002) proposed a technique for conditional monitoring of a turbine blade by using embedded sensors. Ciang *et al.* (2008) compiled a state-of-the-art review of structural health monitoring and damage detection methods specifically for wind turbine applications. In addition, many advanced signal analysis and damage detection algorithms have been developed. For example, Fan *et al*. (2013) proposed a novel transmissibility concept based on a wavelet transformation for structural damage detection of wind turbines.

However, the majority of wind turbine condition monitoring and fault diagnosis techniques use the Fourier transform (FT) or the wavelet transform of the vibration measurement data, which has limitations in dealing with complex response signals in turbine condition monitoring (Ghoshal *et al.* 2000). Therefore, continuous monitoring of rotor blades and timely identification of potential failure become an important issue in preventing failure of the entire wind turbine system.

In this paper, a vibration-based monitoring technique is used to track the geometrical setup of a wind turbine system, which includes the tilt and rolling angles of the blade with respect to the rotation plane. In addition, blade dynamic characteristics during rotation are identified. For tracking the geometrical setup of the blade system during operation, blade vibration data are obtained from a three-axes accelerometer mounted on a single rotating blade. Using blade vibration response measurements, the Rodrigues' rotation formula is applied to transform the data from the sensor coordinate system to the global coordinate system, which provides the modal frequencies of the rotating blades and the geometrical setup of the wind turbine system (i.e., pitch angle and rolling angles). Finally, a subspace identification technique is used to identify the dynamic characteristics of the turbine blades under operating conditions.

2. Experimental setup of rotating turbine blade and tower

A wind turbine system was constructed on a shaking table and subjected to rotation at different speeds and excitation of the tower base. A sketch of the research-scale turbine system is shown in Figure 1. The height of the tower was 3 m and the blade length and width were 80 cm and 20 cm, respectively. The diameter of the rotary blade was approximately 180 cm. The excitation, and thereby the rotation of the turbine blade, was controlled by a motor used to spin the blades at controlled angular velocities. The experiment is characterized by the tower/blade interaction under

blade rotation and tower base excitation. Each blade was equipped with two accelerometers in the flapwise direction (one on the tip of the blade and the other at the middle of the blade). On one of the blade tips, a 3-axes accelerometer (Model 1221, input range ±2 g, Silicon Design, Inc.) was installed instead of a 1-axis accelerometer. The acceleration response data were collected through a wireless communication system at a sampling rate of 200 Hz. Before a dynamic test of the turbine system, an impact loading test on each blade was conducted, keeping the dominant frequency of each turbine blade in the flapwise direction at approximately 3.55 Hz.

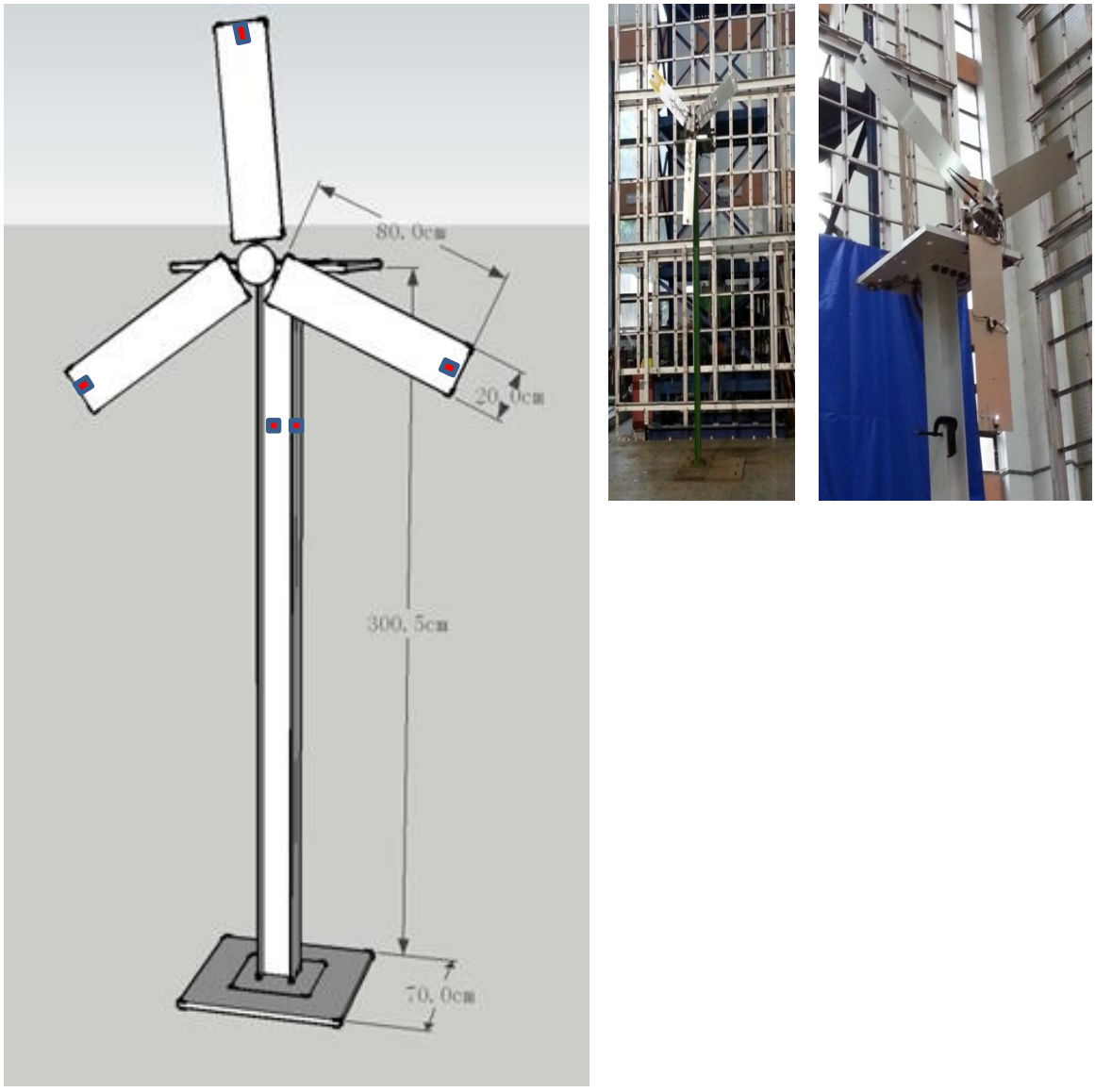

(a) (b) (c)

Fig. 1 (a) Skech of the research-scale wind turbine system and (b) Photos of the turbine systrm mounted on the shaking table

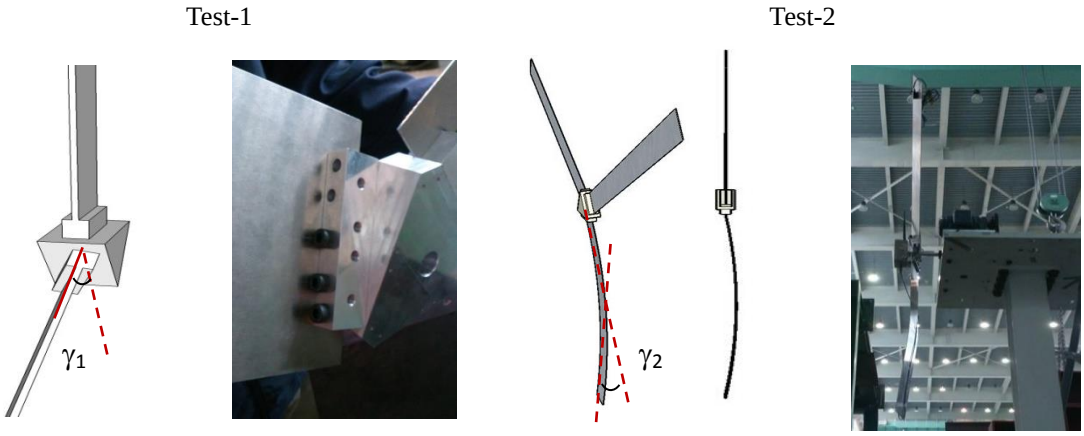

Fig. 2 Sketch and photo of two test cases: In Test-2, rolling angle γ_1 between one blade end and the hub is varied. In Test-3, rolling angle γ_1 is varied similar to Test-2 setup while keeping γ_2 at a fixed value of 12°

For determining the dynamic characteristics of the turbine blade during operating conditions, three test cases were conducted in the laboratory. Each test case setup is described as follows.

- Test-1: Vibration measurements along the flapwise direction of blade motion were collected under rotation frequencies of 15 rpm and 50 rpm. Response measurements were taken from both one 3-axes accelerometer at the tip of a rotating blade and the other five accelerometers (two on each blade along the flapwise motion direction). The connection angles γ_1, γ_2, and γ_3 between the blades and the hub were set at 0°.
- Test-2: Rolling angles between one blade end and the hub were set at $\boldsymbol{\gamma_1}$ = 6°, 10°, and 20° (Type-1, -2, and -3 setups, respectively), as shown in Fig. 2(a), while the other two rolling angles γ_2 and γ_3 were set at 0°. The wind turbine speed was 15 rpm.
- Test-3: Along with varying rolling angle γ_1 similar to Test-2 arrangement (Type-1, -2, and -3 setups with $\boldsymbol{\gamma_1}$ = 6°, 10°, and 20°, respectively), γ_2 was set at 12°, as shown in Fig. 2(b).

Vibration data obtained from Test-1 were used for detecting the flapwise frequency of turbine blades, and the data obtained from Test-2 and Test-3 were used for identifying the geometrical setup of the turbine blade system.

3. Identification of the geometrical setup of the blade using coordinate transformation and the Rodrigues' rotation of measurements

Due to the complicated geometrical setup of the turbine blade system under operating conditions, particularly the tilt and rolling angles, tracking and monitoring of the geometrical setup directly from response measurement becomes a challenge. If the geometrical setup of the rotating turbine blades can be identified under its operating condition, any abnormal condition of the geometrical setup of the turbine system can be detected.

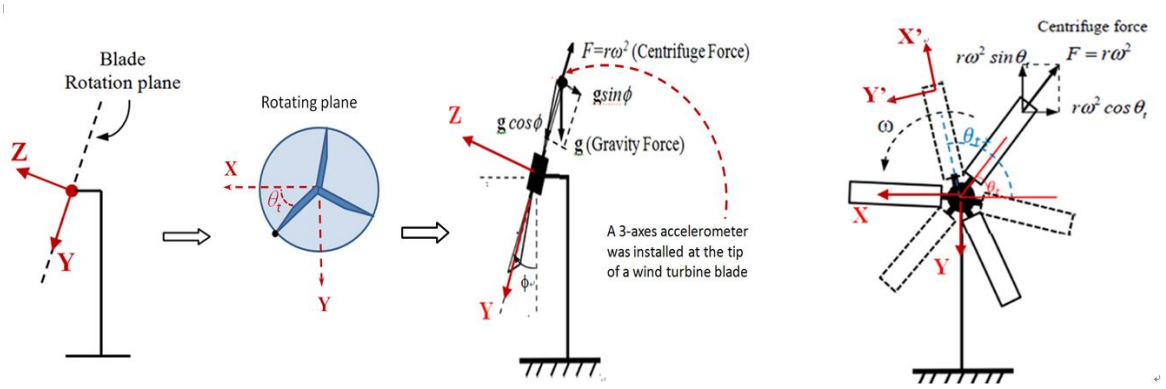

(a) (b)

Fig. 3 (a) A fixed coordinate system defined with the turbine center of rotation as the origin and tilt angle ϕ, (b) The centrifuge force and gravity force acting at the sensing node. The relationship between global and local coordinate systems

3.1 Formulation of the motion of rotating turbine blade system

Let the angle between the blade rotation plane and the direction of gravity be the pitch angle ϕ (Figs. 3(a) and 3(b)). A rectangular coordinate system with the rotating turbine hub as the origin and X-, Y-, and Z-axes along the blade rotation plane is defined as a fixed global coordinate system for the rotation turbine blades. In addition, a local coordinate system with X'-, Y'- and Z'-axes along the radial, tangential, and vertical directions is defined for the location of each 3-axes accelerometer sensing node. During blade rotation, two forces act at the sensing node: the centrifugal force ($F_c = mr\omega^2$) due to the blade rotation with a specific rotation frequency ω and the gravitational force (F_g=mg). First, the centrifugal force is divided into two forces along the fixed global coordinate system at a rotation angle Θ_t: $a_{tx} = r\omega^2 \cos\theta_t$ (along X-axis) and $a_{ty} = r\omega^2 \sin\theta_t$ (along Y-axis). Second, coordinate transformation is applied to the gravitational force and it is expressed in terms of the fixed global coordinate system (along and perpendicular to the blade rotation plane). Therefore, the force vector (or in terms of acceleration, $\{\boldsymbol{a}_t(t,\phi,\theta_t)\}$) in the fixed global coordinate system can be expressed as follows

$$\{\boldsymbol{a}_t(t,\phi,\theta_t)\} = \begin{bmatrix} -a_{tx} \\ -a_{ty} \\ a_{tz} \end{bmatrix} = \begin{bmatrix} r\omega^2 cos\theta_t \\ r\omega^2 sin\theta_t \\ 0 \end{bmatrix} + \begin{bmatrix} 1 & 0 & 0 \\ 0 & cos\phi & -sin\phi \\ 0 & sin\phi & cos\phi \end{bmatrix} \begin{bmatrix} 0 \\ 0 \\ g \end{bmatrix} \tag{1}$$

or

$$\{\boldsymbol{a}_t(t,\phi,\theta_t)\} = \begin{bmatrix} -a_{tx} \\ -a_{ty} \\ a_{tz} \end{bmatrix} = \begin{bmatrix} r\omega^2 cos\theta_t \\ r\omega^2 sin\theta_t \\ 0 \end{bmatrix} + [\boldsymbol{R}] \begin{bmatrix} 0 \\ 0 \\ g \end{bmatrix} \tag{1a}$$

where θ_t is the angle of rotation at any particular time and ϕ is the tilt angle of rotating plane, and r

is the distance between the sensor location and the center of the rotation axis. $[\boldsymbol{R}]$ is defined as the Rodrigues' rotation formula (will be discussed in next section).

The data vector $\{\boldsymbol{a}_{\mathrm{t}}(\mathrm{t},\phi,\theta_{\mathrm{t}})\}$ expressed in the fixed global coordinate system can be transformed to the local coordinate system of the tip of the blade where the sensing node is located (defined by the X'Y'Z' coordinate system) and is represented as $\{\boldsymbol{a}_{\mathrm{t_r}}(\mathrm{t},\phi,\theta_{\mathrm{t}})\}$. Therefore, the relationship between $\{\boldsymbol{a}_{\mathrm{t}}(\mathrm{t},\phi,\theta_{\mathrm{t}})\}$ and $\{\boldsymbol{a}_{\mathrm{t_r}}(\mathrm{t},\phi,\theta_{\mathrm{t}})\}$ can be expressed in the following equation (Fig. 3(b))

$$\{\boldsymbol{a}_{tr}(\mathrm{t},\phi,\theta_t)\}=\begin{bmatrix}-\cos\theta_t & -\sin\theta_t & 0\\ \sin\theta_t & -\cos\theta_t & 0\\ 0 & 0 & 1\end{bmatrix}\{\boldsymbol{a}_t(\mathrm{t},\phi,\theta_{\mathrm{t}})\} \tag{2}$$

Because the sensing node at the tip of one blade also contains the rolling angles, another sensor coordinate system (represented by X''-, Y''-, and Z''-axes) is defined, as shown in Fig. 4. Another coordinate transformation from the local coordinate system to the real sensor coordinate system is required, considering the geometrical setup of the blade. To simplify the geometrical setup, three different types of blade rotations, i.e., γ_{S1}, γ_{S2}, *or* γ_{S3} (rolling angles of the blade) are assigned (Fig. 4). The Rodrigues's rotation formula can be extended to transform all three basis vectors to compute a rotation matrix from an axis–angle representation.

3.2 Rodrigues' rotation formula

The Rodrigues' rotation formula is an efficient algorithm to compute a rotation matrix from a rotation vector in space with a given axis and rotation angle. Murray *et al.* (1994) proposed a robotic manipulation in mathematics, whereby they introduced the Rodrigues' rotation formula, which can be obtained from *MathWorld* by Belongie (1999). The Rodrigues' rotation formula is applied to the acceleration data measured from the rotating turbine blade, discussed as follows. As shown in Fig. 5, consider a vector $\vec{\boldsymbol{x}}$ (representing an axis in the local coordinate system) defined as

$$\vec{\boldsymbol{x}} = a\hat{\boldsymbol{n}}_1 + b\hat{\boldsymbol{n}}_2 + c\hat{\boldsymbol{n}}_3 \tag{3}$$

Let vector $\vec{\boldsymbol{x}}$ be rotated at an angle θ with respect to $\hat{\boldsymbol{n}}_3$; therefore, it can be expressed as

$$\vec{\boldsymbol{x}}' = a\hat{\boldsymbol{n}}_1' + b\hat{\boldsymbol{n}}_2' + c\hat{\boldsymbol{n}}_3' \tag{4}$$

where $\hat{\boldsymbol{n}}_1'$ and $\hat{\boldsymbol{n}}_2'$ are the two new vectors on the plane formed by vectors $\hat{\boldsymbol{n}}_1$ and $\hat{\boldsymbol{n}}_2$ at an angle of rotation θ. The new vector $\vec{\boldsymbol{x}}'$ can be further expressed as

$$\vec{\boldsymbol{x}}' = \cos\theta\,\vec{\boldsymbol{x}} + (\sin\theta)\,\hat{\boldsymbol{n}}\times\vec{\boldsymbol{x}} + (1-\cos\theta)\,\hat{\boldsymbol{n}}\times(\hat{\boldsymbol{n}}\times\vec{\boldsymbol{x}}) \tag{5}$$

Next, defining $\boldsymbol{Nx} = \hat{\boldsymbol{n}}_3 \times \vec{\boldsymbol{x}}$, the relationship between $\boldsymbol{x}$ and $\boldsymbol{x}'$ can be expressed as

$$\vec{\boldsymbol{x}}' = \vec{\boldsymbol{x}} + (\sin\theta)\boldsymbol{N}\boldsymbol{x} + (1-\cos\theta)\boldsymbol{N}^2\boldsymbol{x} \tag{6}$$

The Rodrigues rotation formula can be expressed as

$$\boldsymbol{R} = (\cos\theta)I + (\sin\theta)\boldsymbol{N} + (1-\cos\theta)\boldsymbol{N}^2 \tag{7}$$

Expanding $\boldsymbol{R}$, we can obtain the three-dimensional Rodrigues' rotation formula in the following form

$$\boldsymbol{R} = \begin{bmatrix} cos\theta + n_1^2(1-cos\theta) & n_1n_2(1-cos\theta) - n_3sin\theta & n_1n_3(1-cos\theta) + n_2sin\theta \\ n_1n_2(1-cos\theta) + n_3sin\theta & cos\theta + n_2^2(1-cos\theta) & n_2n_3(1-cos\theta) - n_1sin\theta \\ n_3n_1(1-cos\theta) - n_3sin\theta & n_3n_2(1-cos\theta) + n_1sin\theta & cos\theta + n_3^2(1-cos\theta) \end{bmatrix} \tag{8}$$

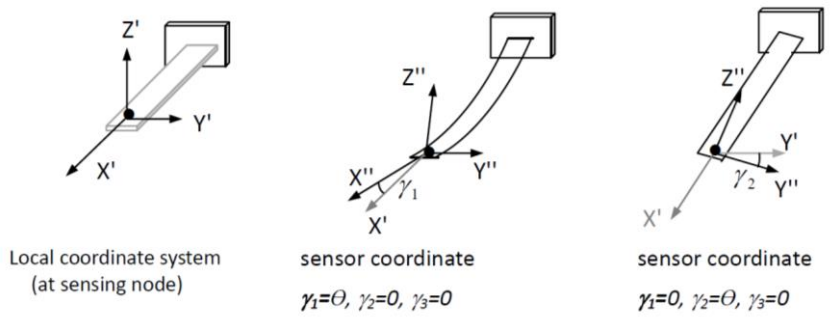

Fig. 4 Three rolling angles γ_{S1}, γ_{S2}, *and* γ_{S3} on sensor coordinate system with respect to blade rotation plane (Local coordinate system)

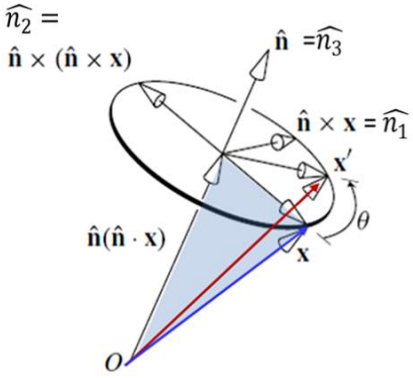

Fig. 5 Concept of Rodrigues' rotation: Rotate a vector **x** on **n**-axis by an angle θ

where θ is one of the rotation angles (i.e., $\gamma_{S1}, \gamma_{S2}, or\ \gamma_{S3}$) , and $\langle n_1, n_2, n_3 \rangle$ is the unit vector in each of the sensing coordinate.

Data collected from the 3-axes sensor mounted at the tip of one of the rotating turbine blades are first represented in the local sensor coordinate system, which is then transformed to the local coordinate system. This represents a rotating force vector to which the Rodrigues' rotation formula can be directly applied. Therefore, the data vector $\{\boldsymbol{a}_{\mathrm{tr}}(\mathrm{t}, \phi, \theta_{\mathrm{t}})\}$, as shown in Eq. (2), needs to be transformed to the real sensor coordinate system through the Rodrigues' rotation formula as follows

$$\boldsymbol{a}_e\left(t, \bar{\boldsymbol{\beta}}\right) = \boldsymbol{R}\left(-\gamma_{s1}, -\gamma_{s2}, -\gamma_{s3}\right) \ \{\boldsymbol{a}_{\mathrm{tr}}(\mathrm{t}, \phi, \theta_{\mathrm{t}})\} \tag{9}$$

where $\boldsymbol{a}_e(t, \bar{\boldsymbol{\beta}})$ is the estimated acceleration response (not including the blade vibration) at the sensing node in the sensor coordinate system at given suitable parameters $\bar{\boldsymbol{\beta}} = \langle \theta \ \gamma_{s1} \ \gamma_{s2} \ \gamma_{s3} \ \phi \rangle$. $\boldsymbol{R}$ is the Rodrigues' rotation formula corresponding to the rotation with respect to the three rolling angles of the blades. Combining Eqs. (7)-(9), the 3-axes motion at the sensor node can be estimated in the sensor coordinate system at given suitable parameters. The estimated response $\boldsymbol{a}_e(t, \bar{\boldsymbol{\beta}})$ is developed considering only gravity and centrifugal force during rotation (i.e., vibration of the blade in the flapwise direction is excluded).

To estimate the parameters $\bar{\boldsymbol{\beta}}$ from the measurements, an objective function is defined that minimizes the error (norm) between the estimated motion $\boldsymbol{a}_e(t, \bar{\boldsymbol{\beta}})$ and the measurement $\boldsymbol{a}_m(t)$

$$J(\bar{\boldsymbol{\beta}}) = \left\| \boldsymbol{a}_e(t, \bar{\boldsymbol{\beta}}) - \boldsymbol{a}_m(t) \right\| \tag{10}$$

In Eq. (10), five parameters need to be determined: Θ_t (blade rotation angle at time *t*), ϕ (tilt angle), and $\gamma_{S1}, \gamma_{S2}, and\ \gamma_{S3}$ (three rolling angles of the blade with respect to the sensor coordinate system). As an initial data vector $\{\boldsymbol{a}_e(t, \bar{\boldsymbol{\beta}})\}$ for the optimization, an initial set of parameters $\bar{\boldsymbol{\beta}}$ together with a set of 3-axes sinusoidal signals is assumed (generally, the turbine rotation frequency is used to generate the signals). Then, the objective function $J(\bar{\boldsymbol{\beta}})$ is minimized to obtain the optimal estimation of modal parameters and the optimal estimation of response time series, $\{\boldsymbol{a}_e(t, \bar{\boldsymbol{\beta}})\}$. Finally, the optimal signal estimation $\{\boldsymbol{a}_e(t, \bar{\boldsymbol{\beta}})\}$ represents the reconstructed vibration signal of the blade at the sensor coordinate system. Note that the estimated signal $\{\boldsymbol{a}_e(t, \bar{\boldsymbol{\beta}})\}$ is derived from the response of blade rotation only, without considering the flapwise blade vibration. Therefore, the residual signal $\boldsymbol{a}_e(t, \bar{\boldsymbol{\beta}}) - \boldsymbol{a}_m(t)$ can be calculated, which reflects the flapwise blade vibration. The identified parameters $\bar{\boldsymbol{\beta}} = \langle \theta \ \gamma_{s1} \ \gamma_{s2} \ \gamma_{s3} \ \phi \rangle$ can provide information on tracking the blade pitch and rolling angles under the operating condition. The residual signal can be used to identify the flapwise vibration frequency of the turbine blades.

4. Vibration-based identification of wind turbine blade

4.1 Results from Rodrigues's rotation analysis

Application of the coordinate transformation and the Rodrigues' rotation formula to the data collected from the rotation turbine blade system described in Section 2 was investigated. The data from Test-2 and Test-3 cases were used. First, to estimate the parameters of Eq. (10), a dataset with a turbine rotation frequency of 15 rpm, corresponding to a time series with a dominant frequency of 0.25 Hz, was assumed. An arbitrary initial phase $\Theta(t)$ was also assumed. Minimization by adjusting the phase $\Theta(t)$ and the parameter vector $\bar{\boldsymbol{\beta}} = \langle \theta \ \gamma_{s1} \ \gamma_{s2} \ \gamma_{s3} \ \varphi \rangle$ on the objective function of Eq. (10) results in the optimal estimate of the response vector $\{\boldsymbol{a}_e(t, \bar{\boldsymbol{\beta}})\}$. Fig. 6(a) shows the comparison of the recorded acceleration and the estimated values with respect to time response at the given rotation frequency of the blade flapwise motion for the Test-2 case. Fig. 6(b) shows the comparison of the final estimation of the time response data and the recorded acceleration after optimization. The difference between the recorded and the optimal acceleration response estimations for the sensor placed at the tip of one rotating blade was extracted, defined as residual signal, as shown in Fig. 6(c). It is observed that the extracted residual vibration signals induced by the rotation frequency of the turbine blade in both radial and tangential directions are not as significant as those in the flapwise direction. Fig. 7 shows the comparison of the residual signal, the recorded response data, and the optimal estimation data from the three directions of the sensor coordinate system at 15 rpm rotation frequency in flapwise direction. The results indicate that the residual signal in the flapwise direction of blade motion is more significant than other directions of blade motion because the vibration of blades in the flapwise direction was more significant than in the edgewise and axial directions during blade rotation.

In addition to the extracted residual signal, the result of optimization can provide the optimal estimation of the three rolling angles of the blades and the pitch angle of the blade rotation plane. The estimated rolling angles (γ_1, γ_2, and $\gamma_3 = 0^o$) for Test-2 and Test-3 are shown in Tables 1a and 1b. The estimated rolling angles and the pitch angle are consistent with the initial setup. A Fourier amplitude spectrum of the residual signal of the blade flapwise direction of motion is obtained for the case of 15 rpm and 50 rpm, as shown in Fig. 8. From this spectrum, we can clearly determine the dominant flapwise vibration frequency of the blade. The calculated flapwise blade vibration frequencies from both test cases are consistent (3.59 Hz from Test-2 and 3.65 Hz from Test-3). Through this analysis, the calculated residual signal can only represent the blade flapwise vibration, while the blade rotation-induced axial and edgewise accelerations are not included in the recorded data. Therefore, this signal can be used to determine the flapwise modal frequency of the blade system by using a single sensor mounted at the tip of one of the turbine blades. Verification of the estimated dominant blade flapping frequency using a stochastic subspace identification method will be discussed in the following section.

4.2 Verification using stochastic subspace identification

To verify the blade flapping frequency obtained through the aforementioned analysis, a vibration-based system identification method was applied to determine the flapwise vibration frequency of the turbine blade from the blade vibration measurement under the operation condition. A multivariate signal processing and system identification technique, frequency domain

decomposition (FDD) and covariance-driven stochastic subspace identification (SSI-COV), were used.

First, the acceleration response measurements of the flapwise vibration of the three rotating turbine blades for Test case-1 with a rotation frequency of 15 rpm and 50 rpm (i.e., six measurements in flapwise direction) were obtained. Then, using the frequency domain decomposition (FDD), proposed by Brinker *et al.* (2000) and Murtagh *et al.* (2005), singular value decomposition (SVD) of the power spectral density (PSD) was carried out. Since the singular values near the resonant frequency are proportional to the PSD of an SDOF system, determining these values can be used as the starting point for modal parameter estimation. Fig. 9 shows the comparison of the distribution of the major SVD values from FDD for the measured data for the cases of 15 rpm and 50 rpm. From the distribution of the singular spectrum, the relation between the dominant frequency of the blade rotation frequency and the double frequency can be identified.

(a) Recorded & initial wave forms (Left:15 rpm; Right:50 rpm)

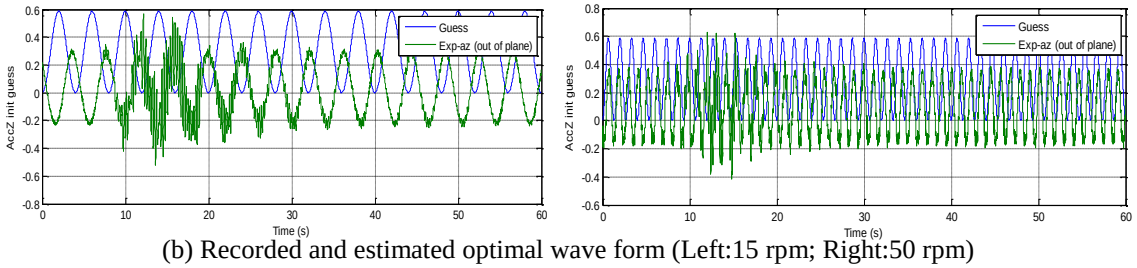

(b) Recorded and estimated optimal wave form (Left:15 rpm; Right:50 rpm)

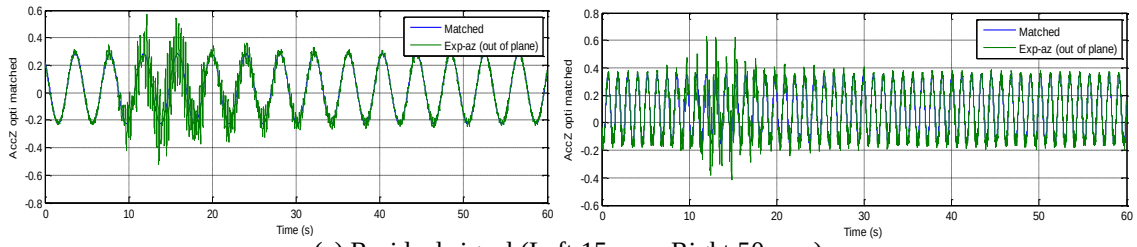

(c) Residual signal (Left:15 rpm; Right:50 rpm)

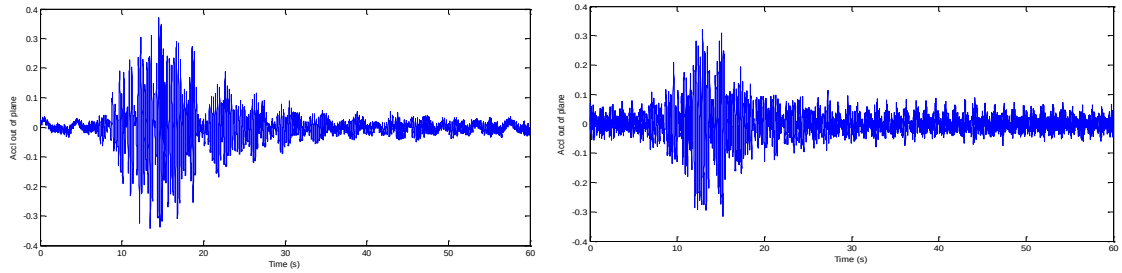

Fig. 6 Plot the comparison of the flapwise motion of turbine blade (test case of 15 rpm and 50 rpm) between; (a) Recorded and initial waveform, (b) Recorded and estimated waveform after Rodrigues' rotation and (c) Residual signal from recorded and estimated waveform

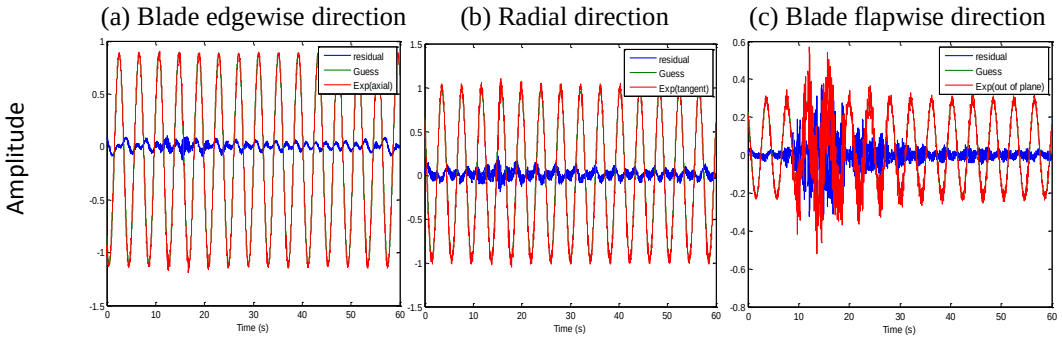

Fig. 7 Plot the calculated residual signal, optimal estimated response signal and recorded signal from three different orthogonal directions of 15 rpm test case; (a) Edgewise direction, (b) Radial direction and (c) Flapwise direction.

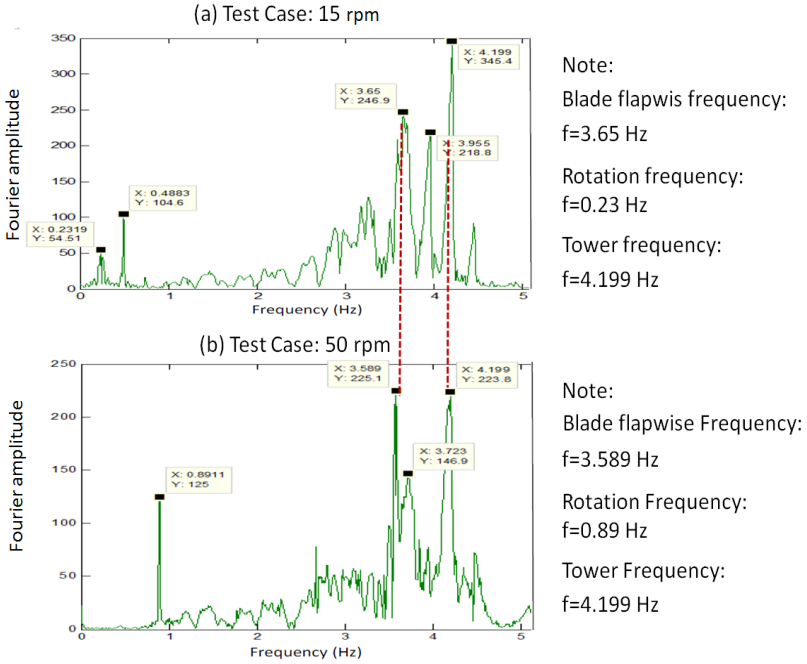

Fig. 8 Fourier amplitude specrum of residual signals of blade flapwise direction ; (a) test case of 15 rpm and (b) test case of 50 rpm

For higher blade rotation frequency, the double frequency is more significant, implying that the response signals from the blade flapwise vibration frequency and the double frequency due to the rotation effect can be observed through FDD analysis. Therefore, using FDD to identify the dominant frequency in the blade flapwise direction alone is impossible.

To solve this problem, the reference-based SSI-COV method, proposed by Bart *et al.* (1999), can be used, which identifies a stochastic state–space model (matrices **A** and **C**) from operation modal analysis (i.e., using output-only data). The stochastic subspace identification (SSI) technique can be applied. The first step is to establish a Hankel data matrix and then form the block Toeplitz matrix from the product of the future and transpose of past measurements. The Toeplitz matrix can be factorized into the extended observability matrix and the reversed extended stochastic controllability matrix. SVD can be used to perform the factorization on the Toeplitz matrix. The observation matrix can be obtained from which the system matrix **A** can be computed by exploiting the shift structure of the extended observability matrix $\mathbf{O}_i$. Finally, the modal frequencies and effective damping ratios can be computed by conducting eigenvalue decomposition of the system matrix **A**. Application of the SSI-COV method together with a data pre-processing technique to the field experimental data has been studied by Loh *et al.* (2012, 2013).

Table 1a Identified wind turbine pitching and rolling angles from Test-2

Test-2	ϕ	γ_1	γ_2	γ_3
15 rpm: Case 1	97.62 (90.0)	-6.78 (-5.0)	-0.35 (0.0)	-0.01 (0.0)
15 rpm: Case 2	89.93 (90.0)	-10.16 (-10.0)	-0.16 (0.0)	0.17 (0.0)
15 rpm: Case 3	96.25 (90.0)	-20.43 (-20.0)	-0.4 (0.0)	-0.15 (0.0)

Table 1b Identified wind turbine pitching and rolling angles from Test-3

Test-3	ϕ	γ_1	γ_2	γ_3
15 rpm: Case 1	89.96 (90.0)	-6.58 (-5.0)	12.81 (10.0)	0.1 (0.0)
15 rpm: Case 2	90.18 (90.0)	-9.6 (-10.0)	12.05 (10.0)	0.63 (0.0)
15 rpm: Case 3	85.1 (90.0)	85.1 (90.0)	10.69 (10.0)	-0.84 (0.0)

Note: (*) indicate the blade rolling angle (degree) in its original setup

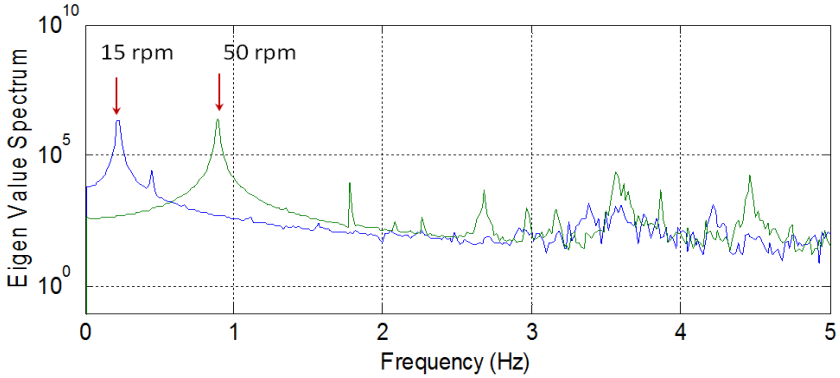

Fig. 9 Plot the singular value distributiom from FDD analysis using 15 rpm and 50 rpm test data

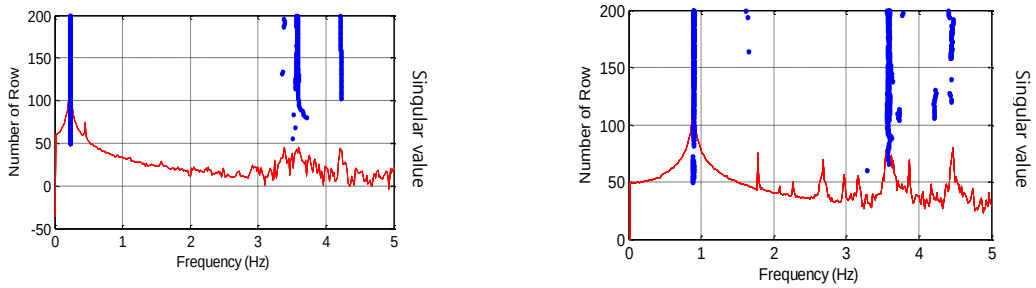

(a) Stability diagram from 15 rpm test data (b) Stability diagram from 50 rpm test data

Fig. 10 The stability diagram from SSI-COV analysis, (a) test case of 15 rpm and (b) test case of 50 rpm. The distribution of singular value from FDD is also shown for comparison

Here, the SSI-COV method was also applied to identify the blade flapwise vibration frequencies. From the stability diagram of the SSI-COV analysis, as shown in Figs. 10(a) and 10(b), the determined rotation frequency and the flapwise blade vibration frequency can be observed. There is no significant difference between the blade vibration frequencies determined in the two test cases. In addition, the tower that supported the turbine blade system with a vibration frequency f = 4.20 Hz can be identified from the 15 rpm test. On the contrary, in the 50 rpm test case, the tower frequency is not so clear in the stability diagram because of the contribution of double frequency. However, from the residual signals, the tower frequency can be determined from both test cases. Comparison between the flapwise blade vibration frequencies determined using the SSI-COV method and the Fourier analysis of the residual signals (through rotation transformation) indicates that the blade vibration frequency, the tower vibration frequency, and the rotation frequency are highly consistent. Using a single 3-axes accelerometer sensor mounted on the tip of a rotating blade and applying the Rodrigues' rotation formula, we can easily determine the flapwise blade vibration frequency and the rolling angles of the blade installation.

5. Conclusions

In this study, a research-scale turbine blade system was used to determine the dynamic characteristics of the turbine blade and track the geometrical setup of the turbine blade system directly from the vibration measurement. The research-scale turbine was rotated using a controlled motor. Through the response measurement, the flapwise vibration frequency of the rotating turbine blade and the rolling angles of the blades could be determined. The turbine blades were equipped with a single 3-axes accelerometer at the tip of one blade, and data acquisition was achieved using a prototype wireless sensing system. The raw data from the test was analyzed to identify the flapwise natural frequencies of the blade. First, the coordinate transformation and Rodrigues' rotation formula were used to track the blade rolling angles and the tilt angle of the turbine blade system through optimization. The proposed method could successfully identify the blade geometrical setup and the residual signals of the flapwise blade response could be used to determine the vibration frequency of the turbine blade. Through this study, the following conclusions are drawn:

1. Application of the Rodrigues' rotation formula to the vibration measurement data results in the flapwise blade vibration signal and the geometrical setup of the blade, such as tilt angle and blade rolling angles. These identified parameters can provide information for turbine blade damage detection through continuous monitoring of the turbine blade system. The advantage of using this method is that data from only one 3-axes sensing accelerometer are required, which can minimize the cost of installation and reduce the computation efforts. Verification of the proposed method in the identification of blade flapwise vibration frequency using a multivariate sensing data through the stability diagrams of the SSI-COV method indicated that the determined blade vibration frequency in the flapwise direction of motion is accurate.

2. It is noteworthy that during the operating frequency of a shaft, synchronous vibration will occur. Synchronous vibration, ω, is the vibratory frequency related to the operating frequency of the shaft. These phenomena need to be carefully examined from the measurement of the rotating wind turbine. By the proposed method of using a single sensor and adopting the Rodrigues' rotation formula as well as the SSI method, the rotational frequency still exists. To remove this rotational frequency, a pre-processing technique through singular spectrum analysis (Loh *et al*. 2013) needs to be applied.

Acknowledgements

The authors gratefully acknowledge the supports from both Ministry of Science and Technology of the Republic of China, Taiwan, under Contract No. MOST 103-2221-E-002 -064 and National Center for Research on Earthquake Engineering on the support of all the testing setup.

References

Barlas, T. and van Kuik, G. (2010), "Review of the state of the art in smart rotor control research for wind turbines", *Prog. Aerosp. Sci*., **46**(1), 1-27.

Bart, P. and Guido, D.R. (1999), "Reference-based stochastic subspace identification for output-only modal analysis", *Mech. Syst. Signal Pr*., **13**(6) 855-878.

Belongie, Serge, *Rodrigues' Rotation Formula*, From *MathWorld*--A Wolfram Web Resource, created by Eric W. Weisstein. http://mathworld.wolfram.com/RodriguesRotationFormula.html.

Brinker, R., Zhang, L. and Andersen, P. (2000), "Modal identification for ambient responses using frequency domain decomposition", *Proceedings of IMAC XVIII*.

Ciang, C.C., Lee, J.R. and Bang, H.J. (2008), "Structural health monitoring for a wind turbine system: A review of damage detection methods", *Measurement Sci. Technol.*, **19** (122001), 1-20.

Fan, Z., Feng, X. and Zhou, Z. (2013), "A novel transmissibility concept based on wavelet transform for structural damage detection", *Smart Struct. Syst.*, **12**(3-4), 291-308.

Ghoshal, A., Sundaresan, M.J., Schulz, M.J. and Pei, F.P. (2000), "Structural health monitoring techniques for wind turbine blades", J. *Wind Eng. Ind. Aerod*., **85**(3), 309- 324.

James III, G.H. (1996), *Development of structural health monitoring techniques using dynamic testing*, SANDIA REPORT: SAND96-0810, UC-706, April.

Lading, L., McGugan, M., Sendrup, P., Rheinländer, J. and Rusborg, J. (2002), Fundamentals for Remote Structural Health Monitoring of Wind Turbine Blades – a Preproject. Annex B – Sensors and Non-Destructive Testing Methods for Damage Detection in Wind Turbine Blades Risø National Laboratory, Roskilde, Denmark.

Loh, C.H., Liu, Y.C. and Ni, Y.Q. (2012), "SSA-based stochastic subspace identification of structures from output-only vibration measurements", *Smart Struct. Syst.*, **10**(4-5), 331-351.
Loh, C.H. and Liu, Y.C. (2013), "Application of recursive SSA as data pre-processing filter for stochastic subspace identification", *Smart Struct. Syst.*, **11**(1) 19-34.
Murray, R.M., Li, Z. and Sastry, S.S. (1994), *A Mathematical Introduction to Robotic Manipulation*, Boca Raton, FL: CRC Press.
Murtagh, P.J., Basu, B. and Broderick, B.M. (2005), "Along-wind response of a wind turbine tower with blade coupling subjected to rotationally sampled wind loading", *Eng. Struct.*, **27**(8), 1209-1219.
Ness, S. and Sherlock, C.N. (1996), *Nondestructive Testing Handbook, Vol. 10*, Nondestructive Testing Overview, American Society for Nondestructive Testing.
Simmermacher, T., James III, G.H. and Hurtado, J.E. (1997), "Structural health monitoring of wind turbines", *Proceedings of the International Workshop on Structural Health Monitoring*, Stanford, CA, September 18-20.